

Supplementary Information

Transparent ITO mechanical crack-based pressure and strain sensor

Taemin Lee,^{†a,b} Yong Whan Choi,^{†a} Gunhee Lee,^{a,b} Peter V. Pikhitsa,^a Daeshik Kang,^c
Sang Moon Kim,^d Mansoo Choi^{*a,b}

^a *Global Frontier Center for Multiscale Energy Systems,
Department of Mechanical and Aerospace Engineering, Seoul National University,
Seoul 151-742, Korea*

^b *Division of WCU Multiscale Mechanical Design, Department of Mechanical and
Aerospace Engineering, Seoul National University, Seoul 151-742, Korea*

^c *Department of Mechanical Engineering, Ajou University, San 5, Woncheon-dong,
Yeongtong-gu, Suwon 443-749, Republic of Korea*

^d *Department of Mechanical Engineering, Incheon National University, Incheon, 406-
772, Korea*

[†]*These authors contributed equally to this work.*

^{*}*To whom correspondence should be addressed. E-mail: mchoi@snu.ac.kr*

Keywords: Strain sensor, Pressure sensor, Transparent, ITO

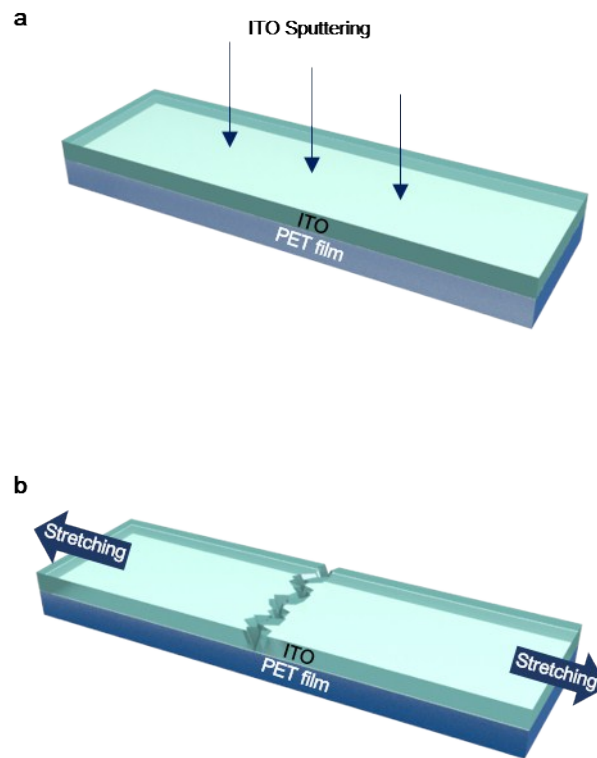


Fig. S1. Fabrication of the ITO crack sensor. (a) ITO layer is deposited by sputtering on PET substrate. **(b)** Strain of 2% is applied to generate cracks on the surface.

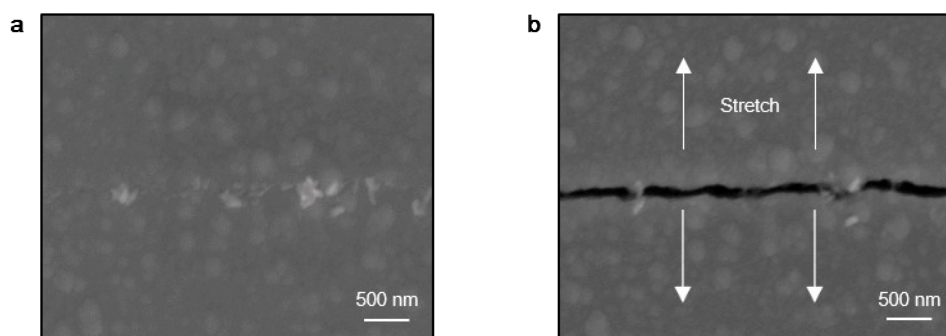


Fig. S2. SEM images of crack opening. (a) SEM image of the crack on the ITO layer with no external tension. **(b)** SEM image of the crack on the ITO layer with strain of 2%.

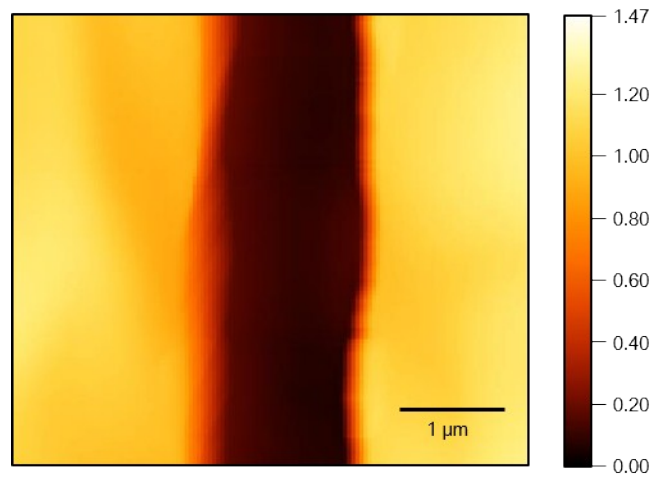


Fig. S3. AFM image of the crack on the ITO deposited PDMS film. The height of the crack is about 1,045 nm.

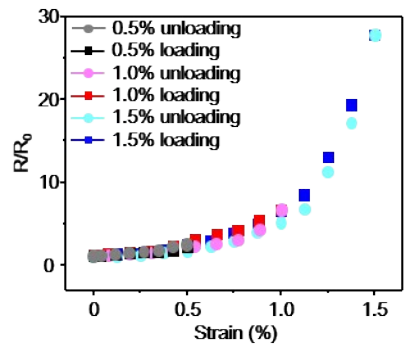


Fig. S4. The graph for loading/unloading tests with the ITO mechanical crack-based sensor with various strains.

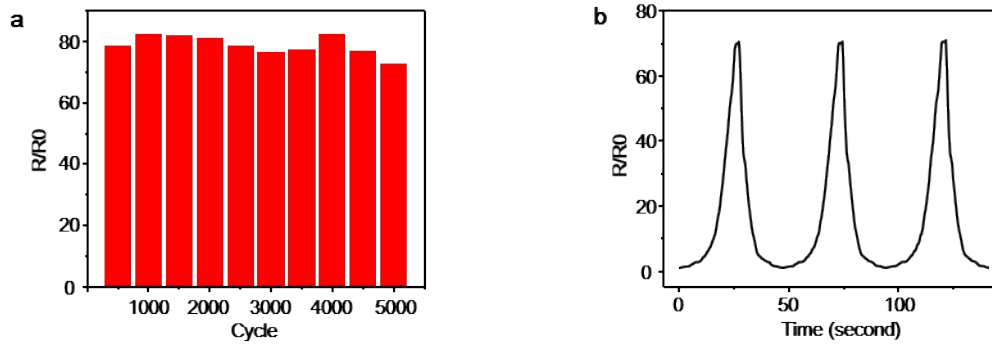


Fig. S5. A marathon test of the ITO crack sensor by repeating loading/unloading process about 5,000 cycles at strain from 0% to 2%. (a) A final normalized resistance of a marathon test at a certain period (about 500 cycles). (b) Loading/unloading test after 5,000 cyclic tests.

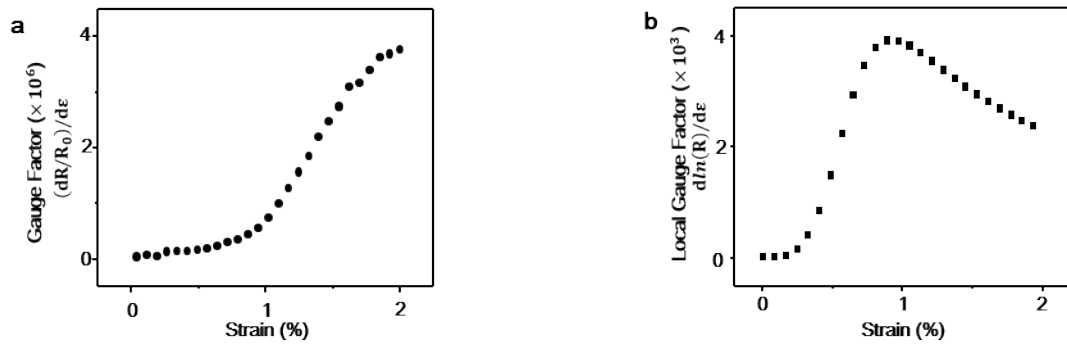


Fig. S6. (a) Strain-dependent gauge factor by taking the derivative of R/R_0 with respect to strains from 0% to 2%. **(b)** Local gauge factor $d\ln(R)/d\epsilon$ versus strains from 0% to 2%.

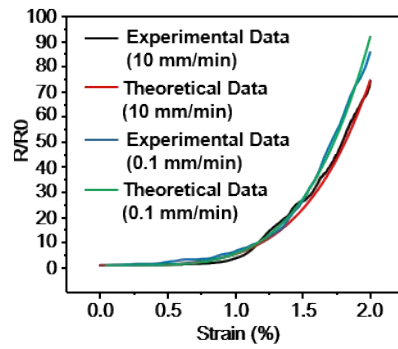


Fig. S7. Loading curves from the ITO crack sensor depending on scanning speeds. The scanning speeds of 0.1 mm/min and 10 mm/min.

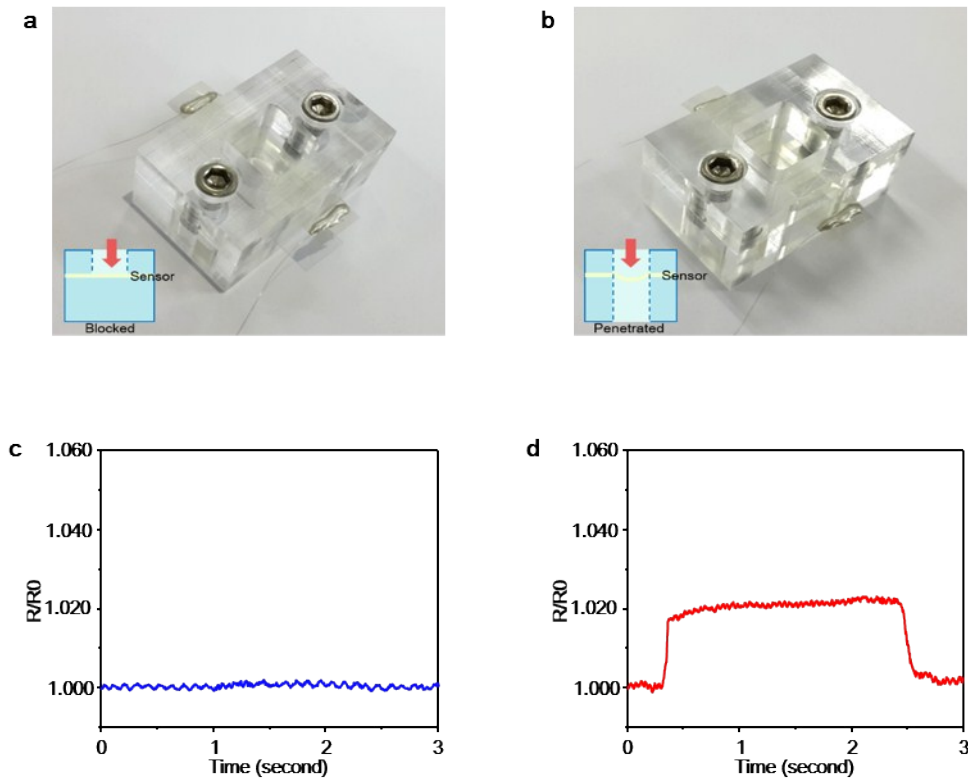


Fig. S8. Pressure and strain sensors depending on the sensor frame structure. (a) Photo image of acrylic frame for strain sensing mode. **(b)** Photo image of acrylic frame for pressure sensing mode. **(c)** Resistance change on the strain sensing mode with vertical pressure (0.15 kPa). **(d)** Resistance change on the pressure sensing mode with vertical pressure (0.15 kPa).

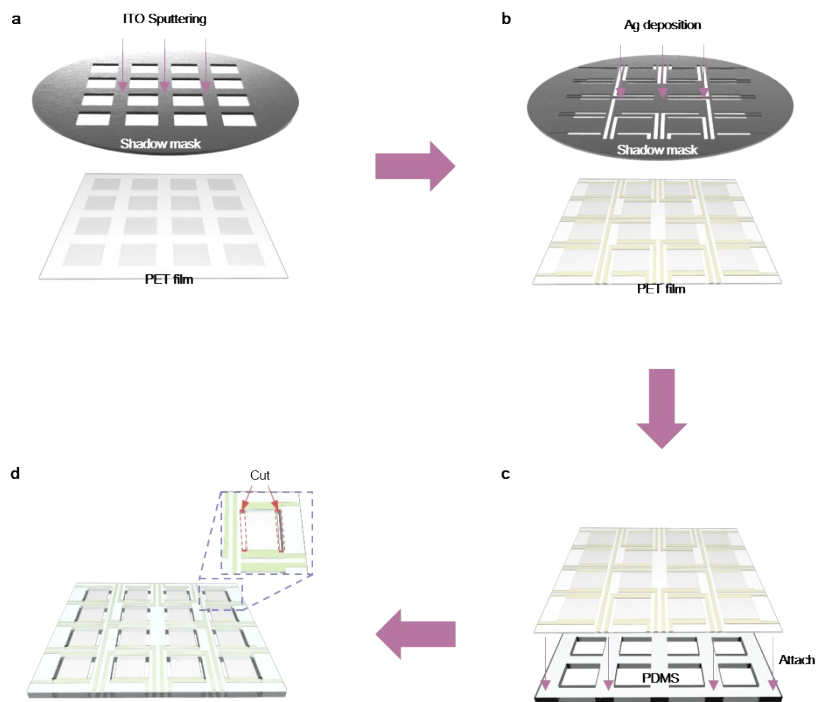


Fig. S9. Fabrication of the multi-pixel array pressure sensor. (a) ITO layer is deposited by a sputter on a PET substrate through a shadow mask. **(b)** Thin Ag metal layer (about 13 nm) is deposited on the ITO layer coated with the PET film by a thermal evaporator through an electrode path shadow mask. **(c)** A PDMS with 4 by 4 square hole is attached on the ITO layer coated with the PET film. **(d)** The edges of each pixel facing each other were cut.

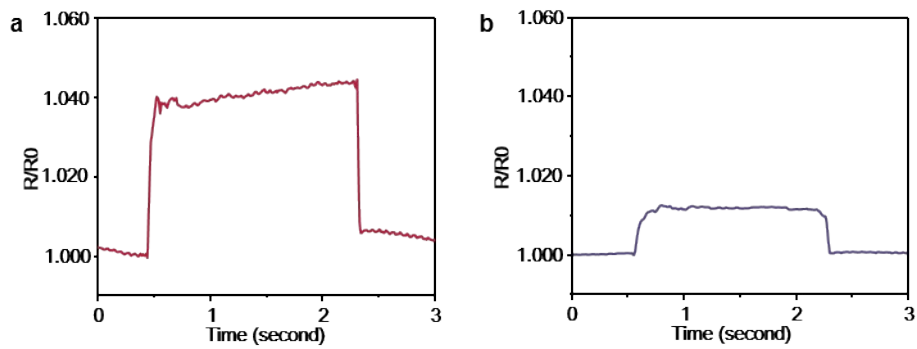


Fig. S10. Normalized resistance changes versus discrete pressure on the multi-pixel array pressure sensor. (a) A response of normalized resistance of 0.176 kPa. **(b)** A response of normalized resistance of 0.12 kPa.